Hindawi
Mathematical Problems in Engineering
Volume 2021, Article ID 9834770, 12 pages
https://doi.org/10.1155/2021/9834770

Research Article

Antiseismic Method of Prestressed Fabricated Building Structure under Intelligent Big Data

Zhonghong Li[1] and Yong Huang[2,3,4,5,6]

[1]*School of Architectural Engineering, Chongqing Chemical Industry Vocational College, Chongqing 401228, China*
[2]*College of Chemistry, Xinjiang University, Urumqi 830000, Xinjiang, China*
[3]*The Province and Ministry Jointly Established the State Key Laboratory of "Carbon-based Energy Resource Chemistry and Utilization", Xinjiang University, Urumqi 830000, Xinjiang, China*
[4]*Xinjiang Communication Construction Co. Ltd (XCCG), Urumqi 830000, Xinjiang, China*
[5]*Transpotation Industry Highway Maintenance Collaborative Innovation Platform under Complicated Conditions of Western China, Urumqi 830000, Xinjiang, China*
[6]*Western Sub-Alliance of Zhongguancun Zhongke Highway Maintenance Technology Innovation Alliance, Urumqi 830000, Xinjiang, China*

Correspondence should be addressed to Yong Huang; yong_huang@seu.edu.mk

Received 27 August 2021; Revised 25 September 2021; Accepted 5 October 2021; Published 8 November 2021

Academic Editor: Sang-Bing Tsai

Copyright © 2021 Zhonghong Li and Yong Huang. This is an open access article distributed under the Creative Commons Attribution License, which permits unrestricted use, distribution, and reproduction in any medium, provided the original work is properly cited.

Compared with traditional buildings, prefabricated buildings have the advantages of simple construction technology, low construction requirements, and shorter construction time, which can generate more economic benefits for the construction industry. In order to study the seismic capacity of prestressed fabricated building structures under intelligent big data, this article takes fabricated frame structures as the research object and the reinforced walls at the nodes as the starting point to study the damage patterns and energy dissipation capabilities of different seismic waves on the structure. In order to observe the overall seismic performance, the fabricated frame structure was used. The results of the study found that the prestressed fabricated building structure has the best seismic effect when the axial compression is 0.3, and the prestressed degree is below 0.5, which meets the seismic requirements. Therefore, the prestressed degree of the prestressed fabricated building structure should be below 0.5. According to statistics on the results of structural residual deformation and steel bar deformation of buildings under different seismic waves, it can be found that the prestressed fabricated building structure has better self-recovery ability and can better respond to earthquakes with different seismic waves.

1. Introduction

With the rapid development of the Chinese economy, people's structural requirements for residential buildings are increasing, and more multistorey residential buildings are available. At present, the main form of high-rise residential buildings in my country is still the cast-in-place concrete frame shear wall structure or pure shear wall structure; this structural form has certain defects from its own point of view [1]. Affected by the environment or the labor level of on-site workers during the construction process, the quality of the construction cannot be well guaranteed. A large number of formworks are required to pour concrete on site, which increases the amount of materials and increases the cost. High-rise residential buildings in our country should move towards fast construction speed, short cycle, low labor intensity, and high degree of industrialization and minimize on-site "wet work," which is helpful to the development of environmental protection and other aspects. In response to these problems, people have gradually realized that

fabricated concrete structures have more advantages than traditional cast-in-place concrete structures [2].

The development of prefabricated buildings has broad market prospects and good policy support in my country. At the same time, the fabricated prestressed concrete shear wall system is formed by combining the fabricated concrete structure with the shear wall system commonly used in residential buildings in my country, which solves the current social problems, such as labor shortage and housing shortage, and compared with the cast-in-place reinforced concrete shear wall, it also has certain advantages in terms of performance, so it has high research value [3]. However, there are also factors limiting the development of prefabricated buildings in my country. Prefabricated structures have a form of building. The prefabricated construction industry chain needs a complete industrial system to support. But the current prefabricated construction system in my country is not perfect and cannot form large-scale production. Transport, assembly, etc. all of this must be solved by us [4].

For prestressed fabricated buildings, experts at home and abroad also have a lot of research. Erhard believed that the minimum reinforcement of the flexurally strengthened masonry should not be less than 0.05 percent of the effective masonry cross section of the building component, in which steel bars contribute to the load bearing capacity of the section, and the effective masonry cross section is the product of the effective width and the building element The usable height d, based on the area of the steel bar, should not be less than 0.03% of the total cross-sectional area, specifying the minimum amount of reinforcement to avoid brittle behavior of the building. When the first crack is formed or limits the cracking element, check the elements given in the minimum number of reinforcement for reinforced masonry beams [5]. Gao tested two prefabricated shear walls with a scale of 50%. One model is that the partially assembled prestressed concrete shear wall unit uses carbon fiber bundles as prestressed tendons and replaces ordinary concrete with reinforced fiber concrete. At the same time, steel plates are installed at the bottom of the wall limbs, and steel diagonal braces are embedded in the prefabricated walls as energy-consuming elements. The connection structure of the simulated cast-in-place assembled shear wall unit can achieve the integrity of the wall and the base, which is basically equivalent to the cast-in-place shear wall, but the residual deformation is large, and the damage is serious [6]. Guéguen et al. conducted an experimental study on the prefabricated hollow wall panel combination. The combination is composed of 2 load-bearing panels at both ends and 4 nonload-bearing panels in the middle. The load-bearing wall panels are connected to the bottom plate through prestressed compression. The load-bearing wallboard is only placed on the bottom plate by rubber blocks, and the rubber blocks form a two-point connection between each wallboard, and the sealant is filled. The test results show that the precast concrete hollow wallboard combination has better lateral resistance [7]. Fujie et al. conducted an experimental analysis on the seismic performance of the in-line, T-shaped, and double-leg prestressed shear walls and compared them with the cast-in-place shear walls. The test results showed that the precast shear walls are in rigidity, yield strength, and ultimate strength. Compared with the cast-in-place shear wall, it is greatly improved, and the ability to resist cracking and elastic deformation is stronger. The damage of the wall is mainly concentrated at the root of the wall and the intersection of the connecting beam and the wall. The whole wall is damaged by bending and shearing. Bending damage is the main cause; energy consumption and ductility are poor. Because the structure itself has good elasticity and self-healing, it is easier to repair after cracking, which has good social benefits [8]. These studies have a certain reference effect for this article, but the sample limit of the study is severe, and it is difficult to reproduce in practice.

This study studies the seismic performance of prefabricated building structures and establishes a prefabricated node model. The establishment of the model needs to consider the influence of factors, such as the selection of cross sections, the characteristics of materials, the division of elements, and the nonlinear analysis. The seismic performance analysis and comparison of the frame structure and the prefabricated building structure are carried out using the dynamic time history analysis method under the same site conditions and the same construction conditions to carry out the quasirare earthquake analysis, which is the prefabricated, prestressed, building structure in the actual project. The application provides suggestions.

2. Seismic Research Methods of Prestressed Fabricated Building Structures

2.1. Prestressed Fabricated Building Structure. The key to the study of prefabricated structures is the study of joint connections. The connection technology is mainly divided into two types: rigid connection and dry connection, which is the basic technology of prefabricated concrete structures [9]. Research through related experiments shows that strengthening the connection at the node can improve the overall performance of the structure, and the precast concrete structure can meet the energy consumption performance requirements.

In order to improve the energy consumption and ductility of the fabricated shear wall and to reduce the horizontal shear slip and the degree of joint opening of the fabricated concrete shear wall, this study proposed two connection methods, one is the bottom cast in place. The upper part adopts the prestressed press-joined assembled shear wall; the other adopts the continuous steel bar with a partially reduced section to transfer the plastic hinge from the splicing joint to the wall, as shown in Figure 1 [10, 11].

Aiming at the problem of poor energy absorption efficiency of constructed concrete shear walls, many studies have introduced energy dispersion elements into fabricated concrete shear walls, such as liquid damping and abrasion damping. This approach is solving energy consumption. Although the capacity is insufficient, it also strengthens the integrity of the walls and reduces the horizontal displacement.

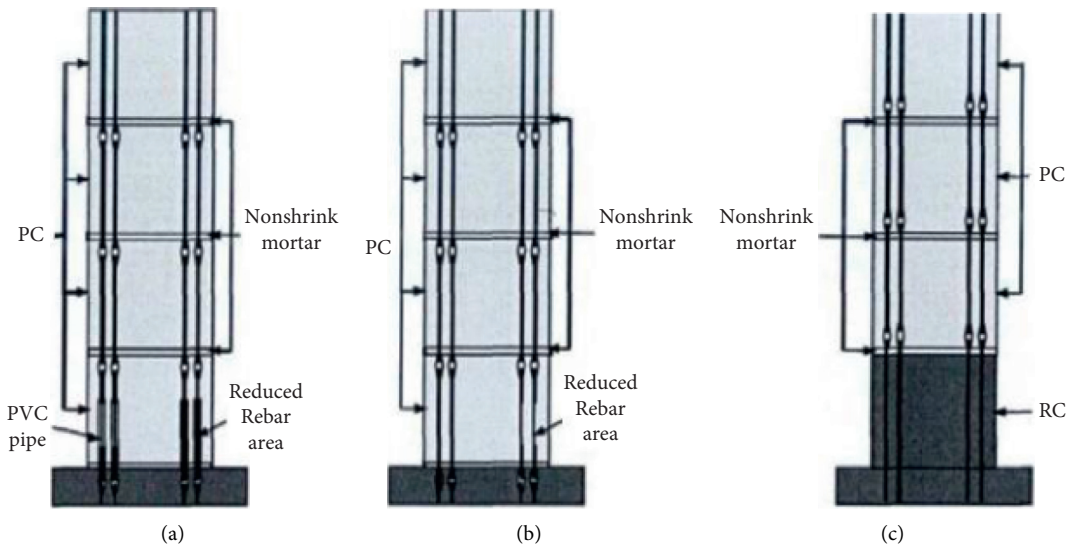

Figure 1: Different base connection methods. (a) PC with unbonded partially reduced rebar area. (b) PC wall with partially reduced rebar area. (c) RC-PC hybrid wall.

Aiming at the problem of poor energy dissipation performance of fabricated prestressed concrete shear walls, many studies have introduced energy dissipation elements into fabricated prestressed concrete shear walls, such as fluid damping and friction damping. This approach is solving energy consumption. Although the capacity is insufficient, it also strengthens the integrity of the walls and reduces the horizontal displacement. This means that ordinary steel rods are added based on the discounted tendons, and the energy absorption efficiency of the discounted concrete bar is improved through the performance of ordinary steel rods. Plain steel rods have a certain length in the nonroofed section. The ordinary steel bars in the bottom layer are moved to the middle of the wall, and the positions of the other layers remain unchanged. The stirrups are also changed from circular spiral stirrups to rectangular closed stirrups to increase large concrete core area [12]. Relevant studies have proved: (1) The main mode of horizontal deformation of hybrid fabricated shear wall is the opening of the gap at the joint, and the shear wall can basically be regarded as a rigid body around the joint. Rotation, the damage degree is obviously lower than that of the cast-in-place shear wall. (2) In the unloading stage, due to the elastic action of the prestressed tendons, the shear wall is provided with a vertical restoring force, which can reduce the residual deformation of the component after the earthquake. (3) The yield of local unbonded ordinary steel bars is obviously lagging behind, which also avoids the occurrence of low-cycle fatigue fracture. The mixed fabricated shear wall and its improved wall are shown in Figure 2:

In summary, our country's research on prefabricated concrete is mainly focused on several specific structural forms such as fabricated frame structure, fabricated concrete shear wall structure, and prestressed fabricated structure [13]. The research on prefabricated concrete shear walls is more about the seismic performance of the joints, whereas the overall seismic research of the structure is less. At present, the three connection methods of corrugated pipe grout anchor lap connection, sleeve grouting connection, and constrained grout anchor lap connection are the most widely used in prefabricated concrete shear walls, and they have achieved rapid promotion and application [14].

2.2. Calculation of Partial Deformation of Building Concrete. We take a prefabricated slab in the floor as an insulator, as shown in Figure 3.

According to the beam theory and the force relationship, the bending angle θ_c under the action of the in-plane bending moment M is obtained as

$$\theta_c = \frac{Mb}{E_c I_c}. \tag{1}$$

Among them, b is the width of the isolator, I_c is the bending moment of inertia in the plane of the isolator, and E_c is the elastic modulus of the concrete. According to the material mechanics shear deformation calculation formula of beam theory, the shear deformation Δc of the concrete floor is calculated as

$$\Delta c = \frac{1.2Vb}{G_c A_c}. \tag{2}$$

According to the mechanical performance test at floor level, the axial force of the cross joints is basically a straight line, except for the anchored joints at the edge of the slab, so the joints can be described by the flat section hypothesis. Under the action of the in-plane bending moment M, the bending angle of the plate seam connector is θ_j. Considering the deformation of the connector under the action of bending moment, according to the balance of the axial tension and pressure of the plate joint connector, it is obtained as follows:

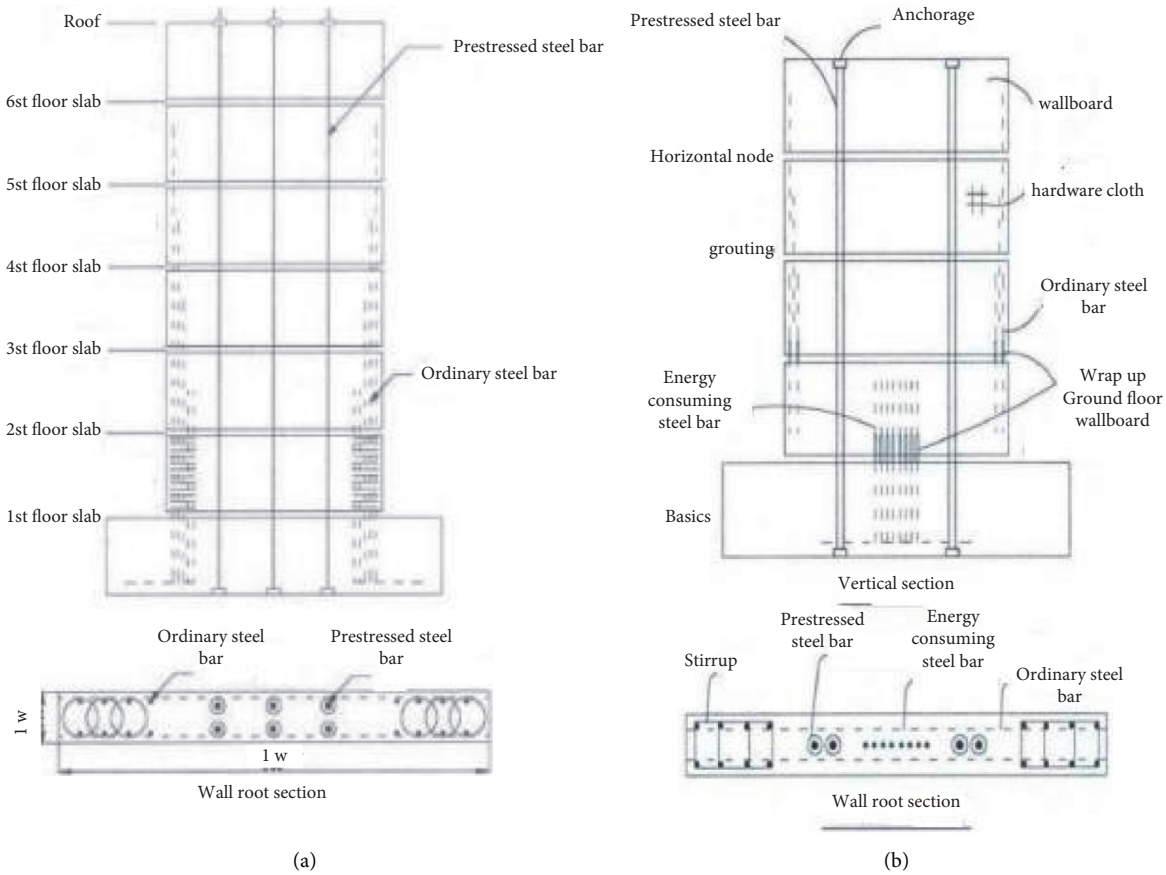

Figure 2: Hybrid fabricated shear wall and its improvement. (a) Hybrid fabricated shear wall system. (b) Improved hybrid fabricated shear wall system.

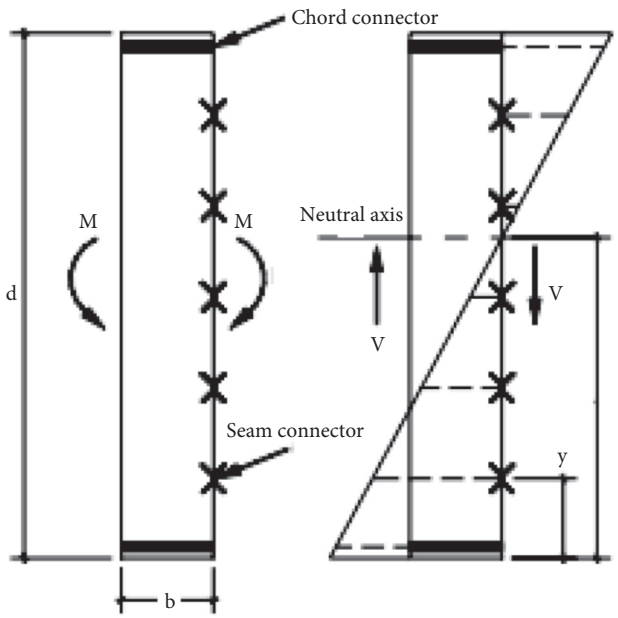

Figure 3: Building isolation layer.

$$\sum_{i=1}^{n} (F_i \delta_i) = 0. \tag{3}$$

Let y be the distance between the section and the wheel and the lower edge of the plate, and y_i is the distance between the i-th joint node and the lower edge of the plate, then

$$\frac{\delta_i}{y - y_i} \tan \theta_j, \qquad \sum_{i=1}^{n} \left[k_i (y - y_i) \tan \theta_j \right] = 0. \tag{4}$$

Available $\tan \theta \neq 0$ from

$$\sum_{i=1}^{n} \left[k_i (y - y_i) \right] = 0. \tag{5}$$

According to the balance of bending moment

$$\sum_{i=1}^{n} M_i = \sum_{i=1}^{n} \left[k_i \delta_i (y - y_i) \right] = \sum_{i=1}^{n} \left[k_i (y - y_i)^2 \tan \theta_j \right] = M. \tag{6}$$

It can be considered that $\theta_j = \tan \theta_j$; therefore,

$$\theta_j = \frac{M}{\sum_{i=1}^{n} \left[k_i^2 \right]}, \tag{7}$$

k_i is the axial stiffness of the i-th connector. The flexural rigidity of the plate seam connector is

$$K_{\theta_j} = \sum_{i=1}^{n} \left[k_i (y - y_i)^2 \right]. \tag{8}$$

According to the axial mechanical balance relationship at the plate seam:

$$\sum_{i=1}^{n} \left[k_i (y - y_i) \right] = 0. \tag{9}$$

This can be transformed into

$$y \sum_{i=1}^{n} k_i - d \sum_{i=1}^{n} \left(\frac{i-1}{m-1} k_i \right) = 0. \tag{10}$$

Therefore, the position of the neutral axis is

$$y = \frac{d \sum_{i=1}^{n} (i - 1/n - 1 k_i)}{\sum_{i=1}^{n} k_i}. \tag{11}$$

Therefore,

$$K_{\theta_j} = \sum_{i=1}^{n} \left\{ k_i \left[\frac{d \sum_{i=1}^{n} (i - 1/n - 1 k_i)}{\sum_{i=1}^{n} ki} - \frac{i-1}{n-1} d \right]^2 \right. . \tag{12}$$

Therefore, the equivalent beam is under the action of uniformly distributed load q and the boundary condition is simply supported: the bending deformation is

$$\chi_1 = \frac{q}{24\mathrm{EI}} \left(l^3 x - 2lx^3 + x^4 \right). \tag{13}$$

The new fully prefabricated building is assembled from multiple prefabricated slabs, and its continuity is not as good as cast-in-situ flooring, so it cannot be considered a homogeneous body for calculating rigidity within the aircraft. We use the equivalent beam model to calculate the midspan deflection, and its deformation includes shear deformation and bending deformation. However, studies have shown that the deformation under horizontal load is dominated by shear deformation, so the midspan deflection deformation can be regarded as the displacement caused by equivalent shear deformation, and the in-plane stiffness of the floor is the equivalent shear stiffness [15, 16].

2.3. Theoretical Analysis Model of Building Seismic Resistance. Compared with cast-in-place slabs, prestressed fabricated building structures have much greater in-plane deformation, and the building cannot be simply regarded as infinite in-plane rigidity. Therefore, a multistory structure composed of prestressed fabricated building structures is constructed. When there is horizontal free vibration or forced vibration under the action of a horizontal earthquake, each floor of the multistory structure undergoes translational vibration and overall rotation at the same time, producing horizontal deformation, so that the lateral displacement value of each vertical member is not the same [17]. Therefore, it is no longer possible to use the "series mass point system" model in the seismic code for structural seismic analysis. Instead, each vertical member should be connected by each layer of semirigid floor to form a space structure. After discretization, a "string" is formed [18].

For the analysis of the spatial structure of the prefabricated structure, this chapter will adopt the mode analysis method based on the response spectrum theory, that is, it will use the free vibration equation of the multiparticle system to solve the physical vibration period and the mode of operation of the structure, and then, using the theory of decomposition and response spectrum acquires the horizontal seismic action of the structure [19]. Comparing the free vibration equation of the "series-parallel multiparticle system" with the free vibration equation of the "series-parallel multiparticle system," it has the following characteristics:

(1) If the vertical bar where the mass point of the two-way shear bar is located, it represents a frame that does not consider the vertical deformation of the bar; the horizontal bar represents the assembled reinforced concrete floor that is regarded as an equivalent shear beam, that is, where the mass point is both the vertical rod and the horizontal rod are shear rods [20]. Then, the restoring force received by the mass point is only affected by the side shift of one mass point up and down and left and right, except for its own side shift. The side shifts of other mass points have no effect on it, as shown in Figure 4(a).

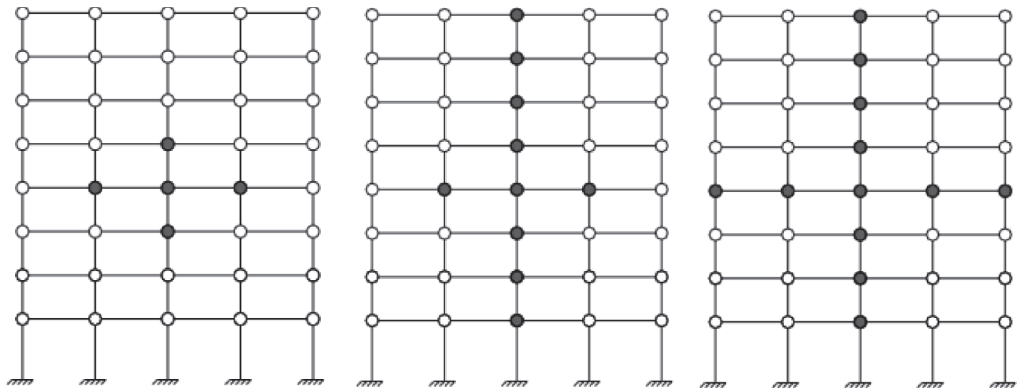

Figure 4: Characteristics of restoring force of series-parallel mass point system. (a) Two-way shear bar. (b) One-way bending shear bar. (c) Two-way bending shear bar.

(2) One-way bending shear bar: If the vertical bar where the mass point is located, it represents the seismic wall belonging to the bending shear type member, and the horizontal bar still represents the prefabricated reinforced concrete floor [21]. Then, the restoring force of this mass point is affected by the side shift of other mass points, the horizontal direction is still one mass point on the left and right, and the vertical direction expands to all the mass points of the vertical rod, as shown in Figure 4(b).

(3) Two-way bending shear bars: if the vertical bar and horizontal bar where the mass point is located represent the seismic wall and the cast-in-place reinforced concrete floor, respectively, they are all bending shear-type members [22]. Then, the range of the side shift of other particles affected by the restoring force of a certain mass point will be further expanded to all mass points where the mass point sits on the vertical rod and the horizontal rod, as shown in Figure 4(c).

The current analysis methods for concrete structures are mainly elastic analysis. However, for the increasingly complex concrete structures, this method appears to be inadequate. Therefore, the nonlinear analysis method has developed rapidly. This method can more fully simulate the behavior of concrete structures under seismic action and has a great effect on the behavior of specific structures under seismic action. For the research and analysis of the seismic performance of traditional concrete structures, there are mainly two types: rod model and story model [23, 24].

The floor model balances the entire structure into a cantilever beam, and each floor is equivalent to a concentrated mass point, and the stiffness is reflected by the steel bars between the mass points. The advantage of this model is that due to the low degree of freedom of the layer model and the low amount of calculation, it can quickly obtain displacement and layer shear, but because the layer model has been greatly simplified, it can only bear the overall seismic structure. Response results cannot reach the results of each component. The calculation results of internal strength and deformation are rough.

We use low-cycle cyclic load to simulate the model, that is, use a specific load test or deformation test to load the sample repeatedly at low cycles to make the sample from the elastic stage to fracture. In the cyclic loading process, the cumulative damage of the components will inevitably lead to a gradual decrease in structural rigidity, weakening of energy consumption capacity, and a degradation phenomenon [25]. Therefore, this decomposition effect of the structure must be considered when creating a restoring force model. The restoring force model is a practical mathematical model obtained by appropriately subtracting and simplifying the relationship between restoring force and deformation obtained from a large number of experiments. It is a concrete manifestation of the seismic performance of structural members in the analysis of structural elastoplastic seismic response. At present, most of the proposed recovery strength models mainly focus on the hysteresis performance under repeated loads. However, for concrete shaft members, due to the large difference in hysteresis between the compression direction and the tension direction, the strength model must be specially studied [26].

3. Seismic Test of Prestressed Fabricated Building Structure

3.1. Model Parameters. To verify the effectiveness of the prefabricated structure analysis, this chapter simulates the cast shear wall test and compares the SAP2000 simulation results with the experimental results. The specific component parameters are as follows: Shear wall concrete: the design is C35 concrete. After testing, the actual compressive strength of C35 concrete is 41.2 MPa, and the thickness of the concrete protective layer is 25 mm. The longitudinal steel bars of the edge members adopt HRB400 hot-rolled steel bars with a diameter of 16 mm. Other vertical distribution steel bars adopt HRB400-grade hot-rolled steel bars with a diameter of 10 mm. The horizontal distribution steel bars adopt HRB400-grade hot-rolled steel bars with a diameter of

10 mm. The stirrups are made of HRB400 hot-rolled steel bars with a diameter of 8 mm. HRB335 grade hot-rolled steel bars. The structural reinforcement diagram is shown in Figure 5. The building wall table is shown in Table 1:

3.2. Prestressed Reinforcement and Nonprestressed Reinforcement. To achieve a good prestress effect, the preoperated tendons must have high strength to ensure high tension is created in the preoperated tendons, thus improving the crack resistance of the preoperated concrete members. The prestressed steel used for prestressed concrete components mainly includes steel yarn, prestressed steel wire, and prestressed spiral steel wire. The nonprestressed reinforcement must be HRB400 and HRB335 steel. In this study, 1860 prestressed steel strands are used to simulate prestressed bars, with a diameter of 15.2 mm and an area of 139 mm^2. The nonprestressed bars are HRB400-grade bars.

3.3. Types of Prestress Loss. The factors that cause the loss of prestress mainly include the following aspects: the shrinkage and creep of concrete cause the prestress loss of the prestressed tendons in the tension zone and the compression zone; the prestress loss caused by the friction between the prestressed tendons and the tunnel wall; during heating and curing, the prestress loss caused by the temperature difference between the tensioned prestressed tendons and the equipment that bears the tension; and the prestress loss caused by the linear prestressed tendons due to the deformation of the anchor and the shrinkage of the prestressed tendons. Due to the discrete nature of the prestress loss, the loss value of the prestress in the actual project may be higher than the loss value calculated according to the specification. Therefore, if the loss value calculated by the calculation is less than the following value, the following value should be selected.

3.4. Statistics. When designing the prestressed tendons of the in-line prestressed shear wall, refer to the general calculation method for the prestressed design of the prestressed concrete shear wall and adopt the value of the effective prestress of the concrete on the wall section to be greater than or equal to the standard value of the concrete tensile strength. The calculation principle is designed and calculated. In the actual project, in order to consider the convenience of construction, the prestressed tendons are arranged in a concentrated manner with bonded prestressed tendons, that is, the calculated prestressed steel strands are arranged in a bundle.

4. Seismic Experimental Analysis of Prestressed Fabricated Building Structure

4.1. Influence of Axial Compression Ratio on Earthquake Resistance. This part studies the effect of axial compression ratio on the seismic performance of prestressed concrete shear walls. By comparing the nonprestressed and prestressed shear walls with different axial compression ratios, the most suitable axial compression ratio for prestressing is studied. In this part, the axial compression ratio of the in-line shear wall is controlled at 0.1, 0.2, 0.3, 0.4, 0.5, and 0.6, respectively, and horizontal load is applied by the method of displacement-controlled loading. The prestress is applied by the cooling method, and the analysis statistics of the next-shaped shear wall with different axial compression ratios without prestress and applied prestress are shown in Table 2:

According to the calculation results in Table 2, when the axial compression ratio of the in-line shear wall is 0.1:0.6, the bearing capacity of the in-line shear wall is increased by 7.5%, 12.7%, and 15.3%, respectively, and the prestressing is increased by 3.5%. When the axial compression ratio is 0.3, the prestressed bearing capacity increases the most. With the increase of the axial compression ratio, the peak load gradually increases. We have also made statistics on the ductility coefficient of the bearing capacity of the structure under different axial compression ratios, as shown in Figure 6:

It is found that the application of gears improves the stiffness and productivity of the wall and reduces the plasticity. The increase of loading capacity and stiffness is more important in low axial compression ratios, so the compression ratio of the axle shaft should not be too high. The axial compression ratio is between 0.1 and 0.3, and the ductility reduction is relatively small. When the axial compression ratio is 0.3, the ductility coefficient is 4.3, which meets the seismic requirements. Therefore, it is recommended that the prestressed axial compression ratio should not exceed 0.3.

Figure 7 shows the wall stress cloud when the steel bar of the prestressed concrete wall under 0.3 yields.

4.2. Influence of Prestressing Tendon Distribution on the Seismic Performance of Walls. Based on the analysis and summary of the axial compression of the in-line shear wall, this section studies the influence of the prestressed tendon arrangement on the seismic performance of the in-line shear wall, and the axial compression ratio is determined to be 0.3. Under the same other conditions, change the way of prestressed tendons. The prestressed tendons are divided into three ways: concentrated on the edge members, concentrated on the middle wall, and evenly distributed on the entire wall, in order to better reflect the influence of the arrangement of different prestressed tendons on the seismic performance of the shear wall. The prestressed tendons are simulated by the distributed arrangement of bonded prestressed tendons. As shown in Figures 8 and 9, the prestressed tendons are concentratedly arranged in the middle wall and uniformly arranged. Schematic diagram of stiffeners scattered throughout the wall. Table 3 shows the statistical results of building analysis of different prestressed tendons.

From the diagram, it can be seen that when the tendon protrusions are concentrated at the ends, their capacity and stiffness are greatest, followed by evenly spaced across the wall and finally concentrated in the middle wall, and the convex tendons are placed at the edge. The time delay of the

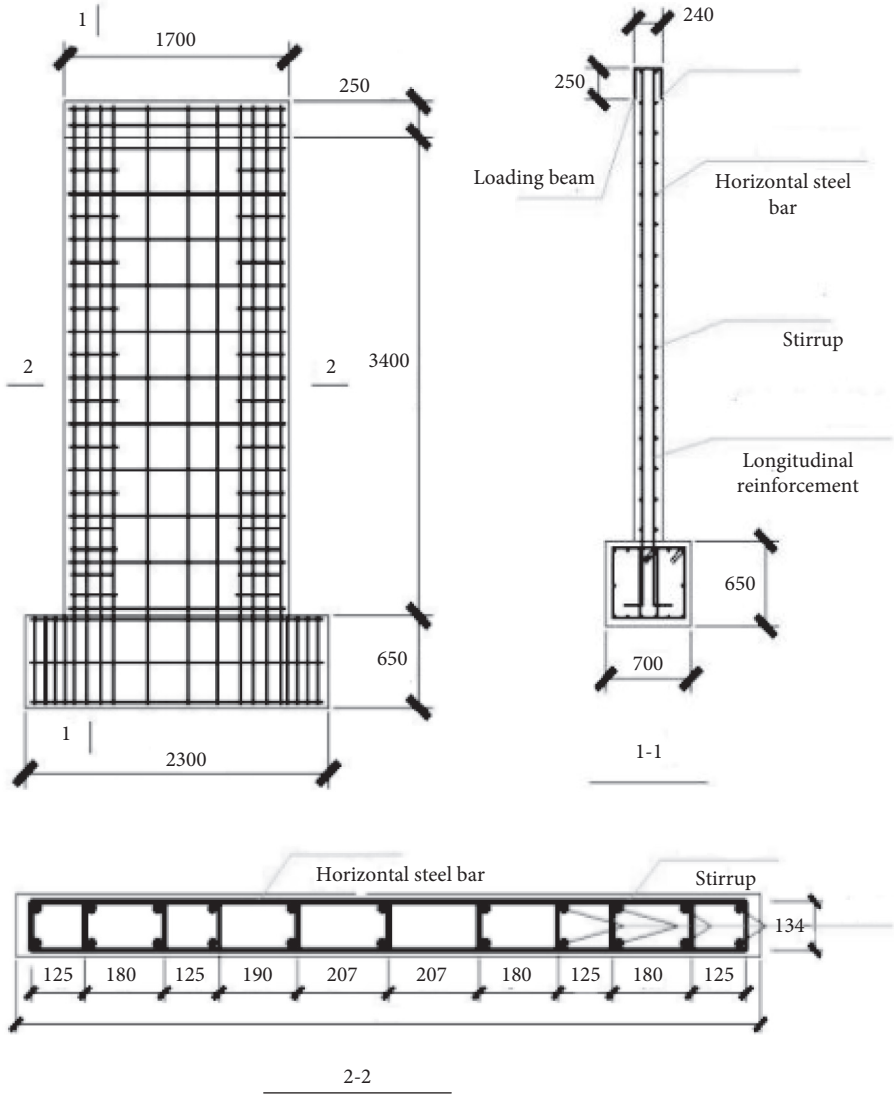

Figure 5: Structural reinforcement diagram.

Table 1: Reinforcement diagram of building structure.

Name	Wall thickness (mm)	Length (mm)	Horizontal distribution rib	Vertically distributed ribs
Q1	200	750	8@200	8@200

Table 2: Statistical results.

Axial pressure ratio	Construct	Yield displacement	Limit displacement	Yield load	Peak load	Ductility coefficient
0.1	No prestressed	3.01	17.7	258	560	5.8
	Prestress	3.13	15.3	316	602	4.8
0.2	No prestressed	2.65	16.8	342	659	4.7
	Prestress	3.21	14.8	380	744	4.5
0.3	No prestressed	3.01	12.6	427	756	4.4
	Prestress	3.35	13.5	488	857	4.2
0.4	No prestressed	3.02	12.5	537	835	4.2
	Prestress	3.84	11.9	536	874	3.2
0.5	No prestressed	2.05	10.2	609	920	3.3
	Prestress	4.01	12.1	567	937	2.7
0.6	No prestressed	3.04	9.8	637	959	3.2
	Prestress	4.09	10.6	599	968	2.6

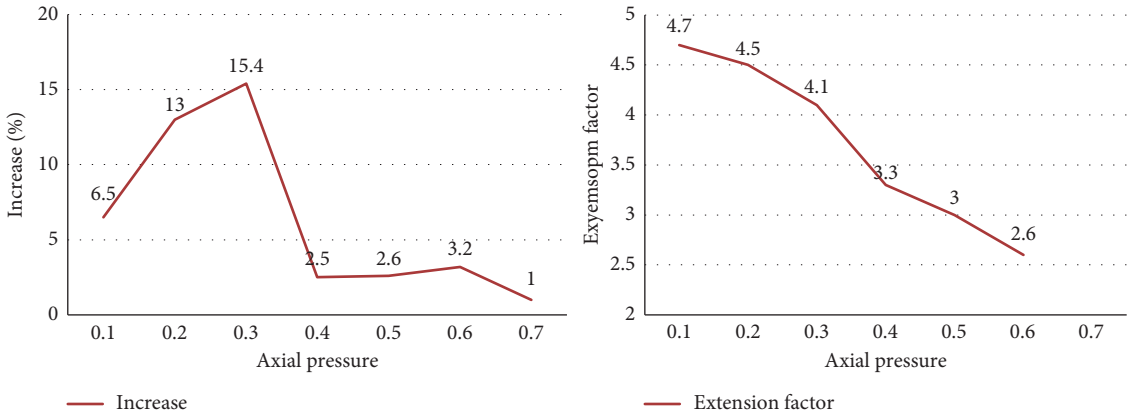

Figure 6: Different shaft compression parameters.

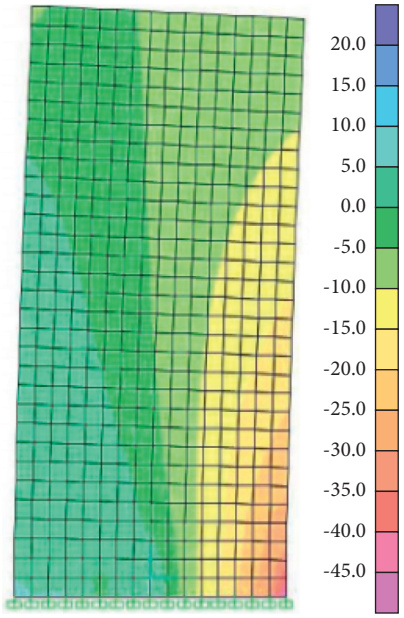

Figure 7: 0.3 axial compression ratio steel bar yield wall stress diagram.

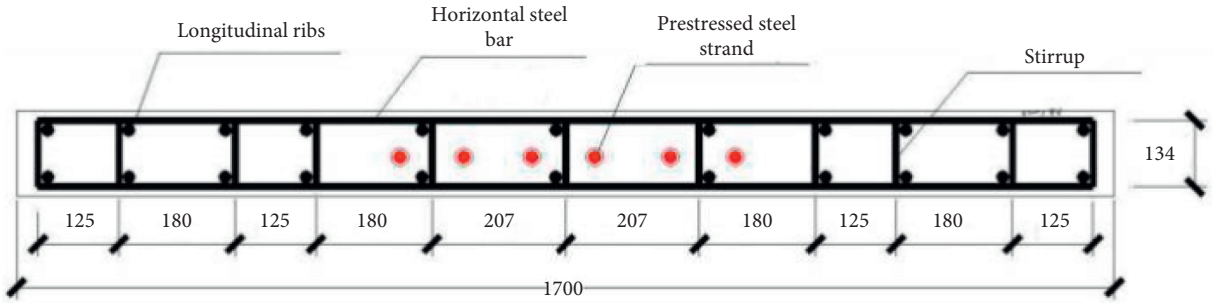

Figure 8: Prestressed tendons are arranged in the middle wall.

component is the worst, but the ductility coefficient is not very different from the other two arrangements. The ductility coefficient is 4.2, which meets the seismic requirements.

We make statistics on the results of structural residual deformation and steel bar deformation of buildings under different seismic waves, as shown in Tables 4 and 5:

It can be seen from the table that under the action of Tafts wave, the entire vibration process of the first floor of the prestressed fabricated building structure is relatively strong, so the residual deformation is relatively insignificant. When the vibration process becomes stable, the displacement curve of the bottom layer is generally concentrated at about 0,

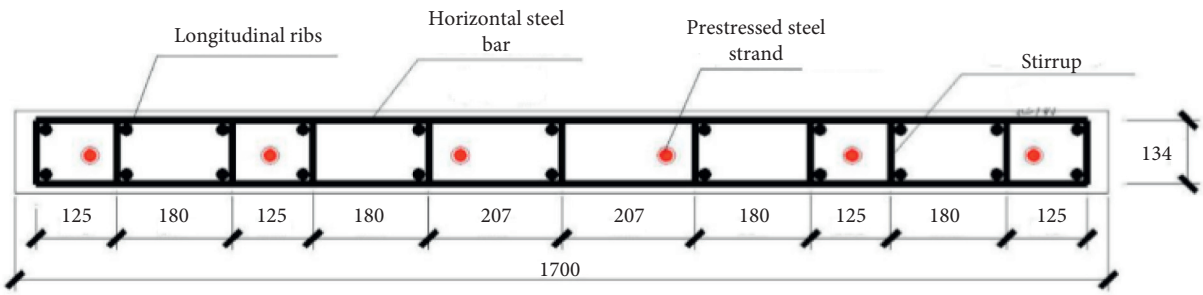

Figure 9: Prestressed tendons are concentrated on the entire wall.

Table 3: Statistical results of building analysis with different prestressed tendons.

Method of prestressed tendons	Yield displacement (mm)	Limit displacement (mm)	Yield load (kN)	Peak load (kN)	Ductility ratio
Focus on edge components	3.26	13.4	489	878	4.2
Distribute the walls evenly	3.07	14.2	427	809	4.5
Centrally arrange the middle part of the wall	2.62	13.2	421	776	4.8

Table 4: Residual deformation under seismic wave.

Residual deformation	Cast in place (mm)	Assembly, 16 mm (mm)	Assembly, 18 mm (mm)	Assembly, 20 mm (mm)
El Centro seismic wave	3	14	0.9	0.4
Tafts seismic wave	2	0	0	0.4
Artificial seismic wave	2	0	0	0

Table 5: Residual deformation of reinforcement under seismic wave.

Residual deformation	Cast in place (mm)	Assembly, 16 mm (mm)	Assembly, 18 mm (mm)	Assembly, 20 mm (mm)
El Centro seismic wave	7	0.54	0.37	0.3
Tafts seismic wave	7.9	0.4	0.24	0.1
Artificial seismic wave	11	1.5	1.3	1.2

which shows the excellent self-recovery ability of the prestressed assembly frame. This is because under the action of seismic excitation, the prestress inside the main beam can forcibly restore the larger deformed beam to its original position. It can be concluded that the seismic performance of the prestressed fabricated frame is higher than that of the traditional cast-in-place frame structure in dealing with the residual deformation of the structure.

On the whole, the residual strain value of the steel bar of the fabricated frame structure is much smaller than the residual strain value of the cast-in-place structure. After comparative analysis, the prestressed fabricated building structure has better self-healing deformation ability. When the seismic grade is level 2, for in-line and T-shaped shear walls, prestress is applied to increase the bearing capacity and rigidity of the shear wall but reduce its ductility. As the prestress degree increases, the rigidity and bearing capacity of the in-line shear wall gradually slow down, and the ductility becomes worse and worse. When the prestress degree is from 0.3 to 0.5, the extent of ductility decline gradually slows down. When the strength is 0.5, the ductility coefficient is 3.46, which meets the seismic requirements. As the prestress degree increases, the stiffness and bearing capacity of the T-shaped shear wall gradually slow down, and the ductility becomes worse and worse. When the prestress degree is from 0.3 to 0.6, the ductility declines slowly and so the prestress degree. When it is 0.6, the ductility coefficient is 6.04, which meets the seismic requirements. Considering the influence of the prestress degree on the bearing capacity, stiffness, and ductility of the shear wall, it is recommended that the prestress degree of the fabricated prestressed reinforced concrete shear wall should not exceed 0.5.

5. Conclusion

Combining a real and regular roof wall structure, this study mainly studies the effect of different axial compression ratios, different preview methods, and different preseismic degrees on the seismic performance of prefabricated building structures. This study designed different parameters, different working condition combinations, established a large number of comparative models for finite element calculation and analysis, and put forward suggestions for the

application of prestressed fabricated building structures in actual projects. Research should be done on the axial compression ratio, different prestressed tendon arrangement methods, and the influence of prestress under different seismic fortification intensity and seismic grade on the seismic performance of shear walls and find out the appropriate axial compression ratio and prestressed tendon layout that can be prestressed. The reinforcement method is used to achieve the appropriate prestress level, but because the content of the analysis is not very comprehensive, only monotonically increasing horizontal force loading is performed, and reciprocating loading simulation is not performed. Therefore, the hysteresis curve cannot be obtained, and the energy consumption structure and performance cannot be analyzed. In addition, it is necessary to compare the seismic analysis of the overall structure with and without prestressing, so as to have a clearer understanding of the seismic performance of the structure.

Data Availability

No data were used to support this study.

Conflicts of Interest

The authors have no potential conflicts of interest in this study.

Acknowledgments

This work was supported by the Scientific Research Youth Project of Chongqing Education Commission (Contract no. KJQN202004502), Natural Science Foundation of Xinjiang Uygur Autonomous Region (General Project, 2021D01A68), Sino-Ukrainian Science and Technology Exchange Project (CU03-32), Hebei Provincial Department of Transportation Science and Technology Project (TH-201918), and Xinjiang Provincial Department of Science and Technology Project (2018E02075).

References

[1] L. Luo, G. Q. Shen, G. Xu, and Y. Liu, "Stakeholder-associated supply chain risks and their interactions in a prefabricated building project in Hong Kong," *Journal of Management in Engineering*, vol. 35, no. 2, pp. 94–107, 2019.

[2] K. M. A. El-Abidi, G. Ofori, S. A. S. Zakaria, and A. R. A. Aziz, "Using prefabricated building to address housing needs in Libya: a study based on local expert perspectives," *Arabian Journal for Science and Engineering*, vol. 44, no. 10, pp. 8289–8304, 2019.

[3] J. G. B. Wesz, C. T. Formoso, and P. Tzortzopoulos, "Planning and controlling design in engineered-to-order prefabricated building systems," *Engineering, Construction and Architectural Management*, vol. 25, no. 2, pp. 134–152, 2018.

[4] G. Tumminia, F. Guarino, S. Longo, M. Ferraro, M. Cellura, and V. Antonucci, "Life cycle energy performances and environmental impacts of a prefabricated building module," *Renewable and Sustainable Energy Reviews*, vol. 92, no. SEP, pp. 272–283, 2018.

[5] G. Erhard, "Minimum reinforcement of beam-type reinforced masonry constructions–proposals for future regulations," *Das Mauerwerk*, vol. 23, no. 4, pp. 209–226, 2019.

[6] H. Gao, "Crustal seismic structure beneath the source area of the Columbia River flood basalt: bifurcation of the Moho driven by lithosphere delamination," *Geophysical Research Letters*, vol. 42, no. 22, pp. 9764–9771, 2016.

[7] P. Guéguen, P. Johnson, and P. Roux, "Nonlinear dynamics induced in a structure by seismic and environmental loading," *Journal of the Acoustical Society of America*, vol. 140, no. 1, pp. 582–590, 2016.

[8] G. Fujie, S. Kodaira, T. Sato, and T. Takahashi, "Along-trench variations in the seismic structure of the incoming Pacific plate at the outer rise of the northern Japan Trench," *Geophysical Research Letters*, vol. 43, no. 2, pp. 228–232, 2016.

[9] X. Chen and C. Liu, "Complex seismic focus structure and earthquake-triggered landslide distribution:analysis of the 2014 ludian M_w6.1 earthquake in Yunnan," *Acta Geologica Sinica*, vol. 2, no. v.91, pp. 365-366, 2017.

[10] K. Wan, S. Xia, J. Cao, J. Sun, and H. Xu, "Deep seismic structure of the northeastern South China Sea: origin of a high-velocity layer in the lower crust," *Journal of Geophysical Research: Solid Earth*, vol. 122, no. 4, pp. 2831–2858, 2017.

[11] M. S. Ekka, V. Ghangas, P. Roy, and O. P. Mishra, "Coda wave seismic structure beneath the Indian Ocean region and its implications to seismotectonics and structural heterogeneity," *Journal of Asian Earth Sciences*, vol. 188, no. Feb., pp. 1–29, 2020.

[12] V. M. Solov'ev, V. S. Seleznev, A. S. Sal'nikov et al., "Deep seismic structure of the boundary zone between the Eurasian and Okhotsk plates in eastern Russia (along the 3DV deep seismic sounding profile)," *Russian Geology & Geophysics*, vol. 57, no. 11, pp. 1613–1625, 2016.

[13] H. Zhu, Y. Tian, D. Zhao, H. Li, and C. Liu, "Seismic structure of the Changbai intraplate volcano from joint inversion of ambient noise and receiver functions," *Acta Geologica Sinica-English Edition*, vol. 93, no. S1, p. 262, 2019.

[14] A. Ohira, S. Kodaira, G. Fujie et al., "Seismic structure of the oceanic crust around petit-spot volcanoes in the outer-rise region of the Japan trench," *Geophysical Research Letters*, vol. 45, no. 20, pp. 123–129, 2018.

[15] Y. Xu, X. Li, and S. Wang, "Seismic structure beneath the Tengchong volcanic area (southwest China) from receiver function analysis," *Journal of Volcanology and Geothermal Research*, vol. 357, no. may15, pp. 339–348, 2018.

[16] C. Jiang, B. Schmandt, K. M. Ward, F.-C. Lin, and L. L. Worthington, "Upper mantle seismic structure of Alaska from Rayleigh and S wave tomography," *Geophysical Research Letters*, vol. 45, no. 19, pp. 350–359, 2018.

[17] T. Ohtaki, S. Tanaka, S. Kaneshima et al., "Seismic velocity structure of the upper inner core in the north polar region," *Physics of the Earth and Planetary Interiors*, vol. 311, no. 1, pp. 106636–106639, 2020.

[18] S. Vijayaraghavan and M. Saimurugan, "Seismic analysis based structure integrity assessment of steam generator in fast breeder reactor," *Materials Today: Proceedings*, vol. 22, no. 4, pp. 3152–3161, 2020.

[19] G. Hou, M. Li, S. Hai et al., "Innovative seismic resistant structure of shield building with base isolation and tuned-mass-damping for AP1000 nuclear power plants," *Engineering Computations*, vol. 36, no. 4, pp. 1238–1257, 2019.

[20] A. Hedayat and M. J. Alborzi, "The seismic analysis of the core structure in a pool-type material test reactor using 3-D finite

difference method," *Progress in Nuclear Energy*, vol. 106, no. jul, pp. 162–180, 2018.

[21] Y. Zhou and Y. Chi, "Seismic noise attenuation using an improved variational mode decomposition method," *Journal of Seismic Exploration*, vol. 29, no. 1, pp. 29–47, 2020.

[22] A. Shito, S. Matsumoto, H. Shimizu et al., "Seismic velocity structure in the source region of the 2016 Kumamoto earthquake sequence, Japan," *Geophysical Research Letters*, vol. 44, no. 15, pp. 7766–7772, 2017.

[23] S.-K Tan, W. Guo, B. Zhou, and S. Han, "Random seismic response analysis of jacket structure with Timoshenko's beam theory," *Ships and Offshore Structures*, vol. 11, no. 3/4, pp. 438–444, 2016.

[24] E. Mistakidis and D. Pantousa, "Fire-after-earthquake resistance of steel structures using rotational capacity limits," *Earthquake and Structures: An International Journal of Earthquake Engineering & Earthquake Effects On Structures*, vol. 10, no. 4, pp. 867–891, 2016.

[25] C. Yong, J. Hu, and F. Peng, "Seismological challenges in earthquake hazard reductions: reflections on the 2008 Wenchuan earthquake," *Science Bulletin*, vol. 63, no. 17, pp. 1159–1166, 2018.

[26] B. B. Gupta, P. Chaudhary, and S. Gupta, "Designing a XSS defensive framework for web servers deployed in the existing smart city infrastructure," *Journal of Organizational and End User Computing*, vol. 32, no. 4, pp. 85–111, 2020.